NANO LETTERS

2007
Vol. 7, No. 8
2214−2219

Assembling Nanowires from Mo–S Clusters and Effects of Iodine Doping on Electronic Structure

P. Murugan,*,† Vijay Kumar,†,‡,⊥ Yoshiyuki Kawazoe,† and Norio Ota§

Institute for Materials Research (IMR), Tohoku University, Aoba-ku, Sendai 980-8577, Japan, Dr. Vijay Kumar Foundation, 45 Bazaar Street, K. K. Nagar (West), Chennai 600 078, India, Hitachi Maxell Ltd., 2-18-2, Iidabashi, Chiyoda-ku, Tokyo 102-8521, Japan

Received March 20, 2007; Revised Manuscript Received June 3, 2007

ABSTRACT

Using ab initio calculations, we find high stability of octahedral Mo_6S_8 clusters, which can further be condensed to form $Mo_{3n}S_{3n+2}$ (*n*, an integer) nanowires. These linear structures are energetically more favorable compared with other closed-packed polyhedral isomers of Mo–S clusters. The octahedral units in nanowires are stabilized by strong Mo–Mo interactions and p–d hybridization between Mo 4d and S 2p orbitals. There is a free electron-like band that crosses the Fermi energy in infinite nanowires and leads to their metallic character. Iodine doping acts as electron donor and can be used to tailor the electronic conductivity. For $Mo_{12}S_8I_4$ nanowires, both electrons and holes are found to contribute to conduction. These nanowires are energetically more favorable than the experimentally obtained $Mo_{12}S_6I_{12}$ nanowires.

Introduction. Currently, there is great interest in understanding the properties of quasi-one-dimensional structures such as nanowires and nanotubes that offer a new paradigm in the design of novel materials as well as opportunities to develop new technologies. In the past two decades, the discovery of carbon nanotubes generated great interest due to their high strength and ballistic transport as well as other novel properties.[1] However, there are difficulties in their usage, as both metallic and semiconducting nanotubes are realized together. For electronic applications, such nanotubes should be separated. Also, carbon nanotubes are often produced in different diameters in the same batch, which could also be disadvantageous in applications due to variation in properties.

Similar to graphite, inorganic fullerene-like and nanotube forms[2−4] have been reported for MoS_2, which also has a layered structure. However, their dimensions are large and the atomic structures have not been well understood. Recently, nanowires of MoS_x doped with iodine have been synthesized both in isolated as well as crystal (bundle) forms.[5−9] The most fascinating aspect of these nanowires is that they have a very small diameter of about 9 Å and can be made with ease in a particular composition such as $Mo_6S_3I_6$ or $Mo_6S_{4.5}I_{4.5}$. Such nanowires therefore have unique properties as compared to carbon nanotubes and can offer an alternative for electric connections at the nanoscale due to their metallic nature. The building block of these nanowires are Mo_6 octahedra that are capped by six S/I atoms, and these units are interconnected with three S/I atoms.[10,11] Therefore, conduction in the nanowire is through the connecting S/I atoms. The connecting atoms lead to unsatisfactory mechanical properties as the Young's modulus of $Mo_6S_3I_6$ nanowire[12] is only 82 GPa compared with the value of 320 GPa for MoS nanowire,[13] which has an infinite chain of connected Mo_6 octahedra.

We therefore consider here MoS nanowires and study the effects of iodine doping on the electronic structure. These are similar to MoSe nanowires that have been synthesized,[14] while crystals of MoS and MoSe nanowires could be produced[15] by doping of alkali atoms with $M_2Mo_6X_6$ (X = S and Se, M = Cs, Na, and K) composition. Recently, such crystals have also been made for $Li_2Mo_6Se_6$ and their transport properties have been measured.[14] In these nanowire-assembled solids, the alkali atom gives charge to the Mo atoms. Another way of achieving similar behavior could be by replacing S with I atoms in MoS nanowires, which will have an effect of reducing charge transfer from Mo atoms. In this letter, we consider this aspect as well as report the stability of the Mo_6S_8 unit and finite nanowires relative to other polyhedral forms having similar compositions. Such finite condensed Mo_6S_8 octahedral clusters are known to exist in a large variety of bulk structures, and their size could be varied depending upon the number of valence electrons

* Corresponding author. E-mail: pmu@imr.edu.
† Institute for Materials Research (IMR), Tohoku University.
‡ Dr. Vijay Kumar Foundation.
§ Hitachi Maxell Ltd.
⊥ Present address: Dr. Vijay Kumar Foundation, 1969 Sector 4, Gurgaon 122001, India.

10.1021/nl0706547 CCC: $37.00
Published on Web 07/11/2007

available for Mo−Mo bonding. It could therefore be possible to prepare different types of Mo−S nanowires by fine-tuning the concentration of the dopants.

Computational Approach. We use an ab initio ultrasoft pseudopotential plane wave method[16,17] and the generalized gradient approximation[18] for the exchange-correlation energy. Clusters and finite nanowires are treated by taking a cubic supercell with large enough lattice spacing so that there is at least 10 Å vacuum space in between the atomic surfaces in neighboring cells. Large-sized nanowires are placed diagonally in the supercell to reduce calculations. Infinite nanowires are modeled by considering 24 atoms with $MoS_{1-x}I_x$ stoichiometry in the supercell along the z direction, which is taken as the nanowire axis. Sufficient vacuum space is left in the x and y directions. The Brillouin zone of the supercell is sampled by the Γ point for clusters and finite nanowires, while 10 k-points are used along the z-axis for the infinite nanowires. The unit cell length along the infinite nanowire axis is optimized and the ions are fully relaxed without any symmetry constraint using the conjugate gradient method. The cutoff energy for the plane wave expansion is taken to be 198 eV in all cases. The convergence is considered to be achieved when the absolute value of the force on each ion is ∼0.005 eV/Å. In many cases, the convergence is better than this, and for smaller size clusters, the convergence on force is ∼0.001 eV/Å. Further studies have been done to check the occurrence of magnetism in finite and infinite nanowires, as some of the Mo−S clusters have been shown to be magnetic.[19] However, we find no magnetic moment on finite and infinite nanowires.

Results and Discussions. As Mo_6S_8 units are abundant in many bulk structures, we consider a few clusters with compositions lying close to that of Mo_6S_8 in order to understand its stability. Some possible structures are based on a Mo_6 prism, Mo_8 cube, as well as Mo_8 tetragonal and Mo_{10} pentagonal antiprism arrangements. These choices are also based on our experience in understanding the structures of Mo_nS_m clusters in which S atoms cap edge, face, or terminal sites of an Mo_n polyhedron. In general, terminal sites for S capping have been found to be quite unfavorable.[19−20] We compare the energies of such structures with the value for the octahedral Mo_6S_8. The optimized structures are shown in Figure 1 and their properties are given in Table 1. The binding energy per atom (BE) is calculated from $BE = (nE(Mo) + mE(S) - E(Mo_nS_m))/(n + m)$, where $E(Mo_nS_m)$, $E(Mo)$, and $E(S)$ are the total energies of Mo_nS_m cluster, an Mo atom, and a sulfur atom, respectively. It is found that the BE is the highest for the Mo_6S_8 (Figure 1a) cluster. A face-capped prism structure of Mo_6S_5, as shown in Figure 1c, has 0.69 eV/atom lower BE, while for an edge-capped octahedron, Mo_6S_{12} (Figure 1b), it is lower by 0.46 eV/atom. The latter is half-metallic and has a magnetic moment of 2 μ_B. The BE of this isomer is even lower than an Mo_6 ring isomer mentioned in ref 19. Also the BE of an edge-capped prism Mo_6S_9 (Figure 1d) is 0.21 eV/atom lower than Mo_6S_8. Even larger clusters of Mo such as Mo_8 and Mo_{10} capped with S atoms (Figure 1e,f) have lower BE (see Table 1). In general, the BE is expected to increase with an increase in cluster size. These results as well as earlier studies[20] on Mo−S clusters suggest that Mo_6S_8 unit is optimally bonded in this size range and this supports the prominent existence of Mo_6S_8 clusters in a large number of Chevrel phase compounds[21] as well as similar units in nanowires.[22] A dominant feature of the most stable structures is the occurrence of a core of metal atoms[19] that is surrounded by S atoms. To further understand the quasi-one-dimensional growth based on octahedral Mo_6S_8 and condensed clusters, we considered stacking of Mo_3 units in octahedral arrangement to form finite nanowires $Mo_{3n}S_{3n+2}$ ($n = 2-10$), which are also capped at both the ends with S atoms (Figure 1g). Capping at the ends increases the BE of the finite nanowires. As an example, there is a gain of 0.21 eV/atom by capping two opposite faces of Mo_6S_6. The BE of the nanowires increases monotonically with length, as shown in Figure 2. The HOMO−LUMO gap of Mo_6S_8 cluster is the largest

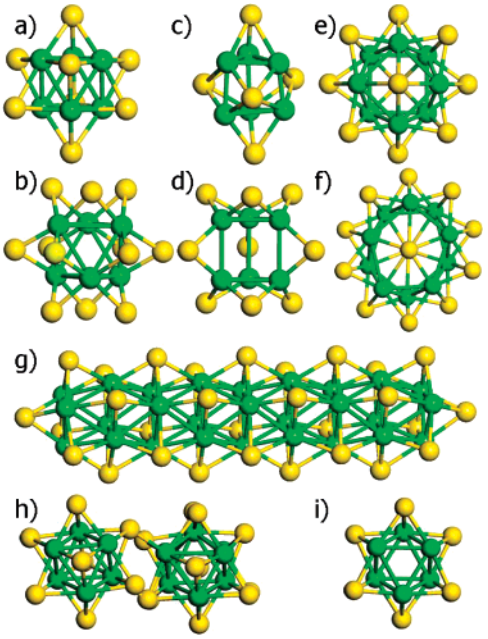

Figure 1. Relaxed structures of (a) Mo_6S_8, (b) Mo_6S_{12}, (c) Mo_6S_5, (d) Mo_6S_9, (e) Mo_8S_{10}, and (f) $Mo_{10}S_{12}$ clusters. (g) A representative optimized structure of the finite $Mo_{3n}S_{3n+2}$ nanowire. Here $n = 9$ nanowire is shown. (h) Optimized structure of $Mo_{15}S_{19}$ cluster obtained from interaction between a Mo_6S_8 cluster and a Mo_9S_{11} finite nanowire. (i) Symmetrical view along the axis of infinite MoS nanowire. Mo (S) atoms are shown by green (yellow) balls.

Table 1. BE and HOMO−LUMO Gaps of Selected Mo_nS_m Clusters

cluster	structure	BE (eV)	gap
Mo_6S_5	face-capped prism	4.13[a]	0.41
Mo_6S_8	face-capped octahedron	4.81	0.91
Mo_6S_9	edge-capped prism	4.60	0.35
Mo_6S_{12}	edge-capped octahedron	4.35	HM[b]
Mo_8S_6	face-capped cube[c]	4.19	0.42
Mo_8S_{10}	face-capped tetragonal antiprism	4.77	0.37
$Mo_{10}S_{12}$	face-capped pentagonal antiprism	4.64	0.33

[a] Partially relaxed; complete optimization resulted into Mo_6 octahedron whose BE is higher by 0.38 eV/atom. [b] Half-metallic (HM) with a magnetic moment of $2\mu_B$. [c] Relaxed structure is given in Figure S1 (Supporting Information).

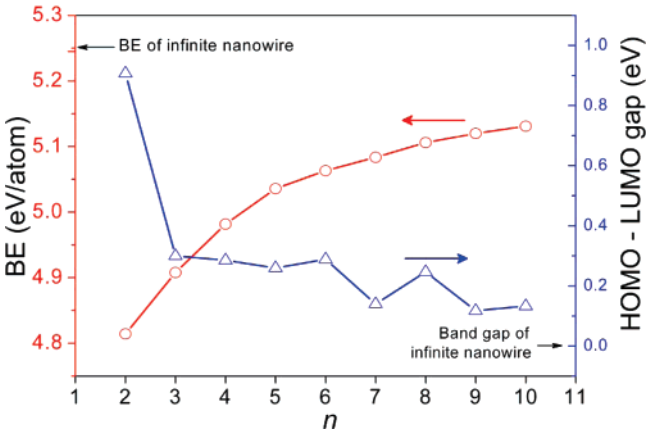

Figure 2. Variation in the BE and HOMO−LUMO gap of $Mo_{3n}S_{3n+2}$ finite nanowires as a function of n. The infinite nanowire is metallic.

among all the clusters considered here and for nanowires it decreases rapidly as more Mo_3S_3 units are added. There are small oscillations in the gap with increasing length due to the quantum size effects and for $n = 9$, the gap has already become quite small. In the limit $n \rightarrow \infty$ (infinite nanowire), the stoichiometric ratio of S:Mo approaches 1:1 and the nanowire is metallic, similar to the result obtained earlier for MoSe nanowires.[14,23] We also examined the linkage between $n = 2$ and $n = 3$ finite nanowires (Mo_6S_8 and Mo_9S_{11}) through the Mo atom of the former and the S atom of the latter and vice versa (see Figure 1h). This fused structure of $Mo_{15}S_{19}$ is found in bulk $Cs_2Mo_{15}S_{19}$ phase.[21] However, its BE (4.93 eV/atom) is lower compared with the value of 5.03 eV/atom for the $Mo_{15}S_{17}$ nanowire. This result suggests that continuous linear growth is favorable and assemblies of clusters and finite nanowires may be stabilized by the presence of Cs atoms.

Further support for the linear structures has been obtained from studies on a $Mo_{12}S_{14}$ cluster with a core of a cuboctahedral Mo_{12} polyhedron, whose fourteen faces are capped by S atoms (relaxed structures are given in Figure S1, Supporting Information). This has the same stoichiometry as $n = 4$ finite nanowire. However, its BE (4.84 eV/atom) is lower compared with the value of 4.98 eV/atom for the nanowire. We also considered placing an atom at the center of the Mo polyhedron with $Mo_{13}S_{14}$ composition. However, the BE is still lower (4.94 eV/atom). These results again suggest that a nanowire structure of $Mo_{12}S_{14}$ is most favorable. Often, in metallic clusters, a close-packed structure[24] with 13 atoms is favored, and in Mo−S clusters, the higher stability of linear structures is due to the interactions with S atoms. It is also striking that a bulk Mo−S compound $K_2Mo_9S_{11}$ has Mo_6S_8 and $Mo_{12}S_{14}$ finite nanowire units, while an antiprism infinite nanowire stacking of Mo_3 clusters is found in the KMo_3S_3 phase.[22]

To get further insight in to the bonding behavior as well as the electronic properties of the infinite MoS nanowires, we have shown the total density of states (DOS) in Figure 3. The typical features of a quasi-one-dimensional structure and van Hove singularities can be noted. There is a finite DOS at the Fermi energy (E_F) and a pseudogap feature (region of low DOS) in the energy range of ~0.5−1.5 eV above the E_F. These results suggest that the properties of such nanowires can be manipulated by doping such that some of the energy states above E_F are occupied and the E_F is shifted to the pseudogap region. To occupy such states, iodine atoms are substituted in place of S in the MoS nanowire. Iodine and sulfur atoms have nearly the same Pauling electronegativity (2.5).[25] We studied $MoS_{1-x}I_x$ nanowires with iodine doping of up to 33.3% by replacing one, two, three, and four S atoms in the unit cell such that no two iodine atoms were nearest neighbors (see Figure S2 in Supporting Information for the structure). The nearest-neighbor configurations were tried but were found to be unfavorable. The resulting optimized structures keep the core Mo nanowire nearly intact while there are small changes in the interatomic bond lengths due to the larger ionic radius of iodine as well as changes in the charge transfer and hybridization. As iodine concentration is increased, the charge transfer from Mo atoms is reduced because iodine prefers one negative charge (I^{1-}), while for sulfur, the S^{2-} configuration is generally favored. Therefore, with iodine doping, more 4d states of Mo are occupied, which results in a shift of the E_F upward (Figure 3). For $x = 25\%$, the E_F shifts to the position where the pseudogap region just begins and this may lead to the electronic stability of this infinite nanowire. With increasing x, the hybridization of Mo orbitals with those of sulfur is affected significantly. The width of the occupied energy bands increases due to the higher contribution from the nearly occupied iodine 5p states, as seen in Figure 3.

The partial DOS of the $MoS_{1-x}I_x$ nanowire with $x = 8.3\%$ is shown in Figure 4. It can be noted that there is a strong hybridization between 3p S and 4d Mo states in the energy range of about −5.3 to −2 eV. Above this energy range, the main contribution to DOS arises from the Mo 4d states. The iodine states lie in the lower part of the spectrum and have weaker hybridization. We further calculated the angular momentum decomposed DOS to find the orbitals involved in the hybridization, and these are shown in Figure S3 (Supporting Information). In the cubic structure of Mo_6S_8, Mo atoms are at the face-centered positions, and for each Mo, the lobes of one of the t_{2g} 4d orbitals point toward S atoms, leading to the p−d hybridization. The lobes of the other two t_{2g} 4d orbitals point toward neighboring Mo atoms and have strong d−d hybridization, while e_g states hybridize weakly. The resulting features can be seen in the angular momentum decomposed DOS in Figure S3. However, in the case of nanowires, one of the t_{2g} type orbitals is constraint in making the p−d hybridization due to the stacking of Mo_3 triangles. It can be seen in Figure S3 that the contribution from the d_{xy} orbital is weaker. States near the E_F arise predominantly from the e_g type orbitals and contribute to the conduction in these nanowires. The doping with iodine will therefore have a significant effect on the transport properties. In Figure 4 (inset a), we have shown the cross section of the electronic charge density distribution in a plane passing through the axis of the nanowire. There is high density around S atoms while there is relatively lower density around Mo atoms, which is expected due to charge transfers.

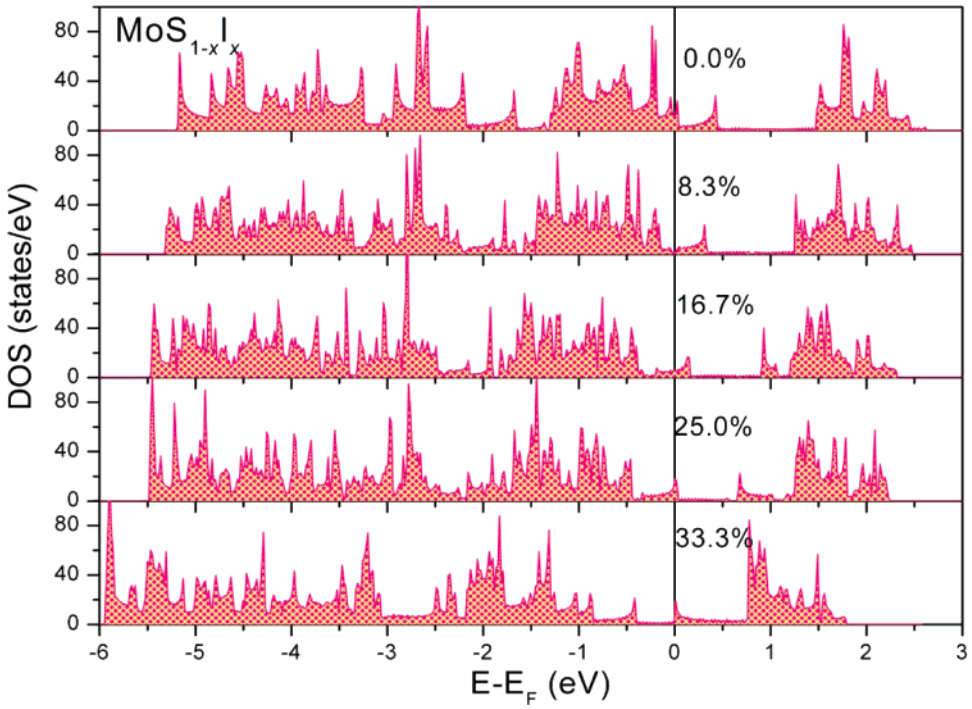

Figure 3. Total DOS of infinite $MoS_{1-x}I_x$ nanowires with $x = 0$, 8.3, 16.7, 25, and 33.3%. It shows that the E_F shifts toward a pseudo gap region by the addition of iodine atoms.

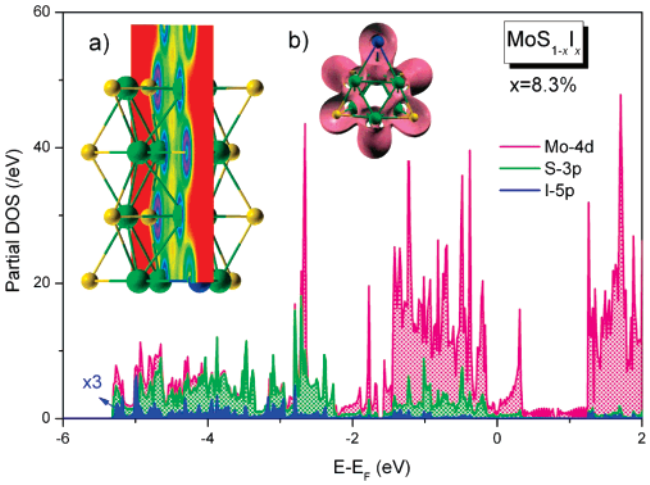

Figure 4. Orbital decomposed DOS for $MoS_{1-x}I_x$ nanowire with $x = 8.3\%$. Inset (a) shows a cross section of the total electronic charge density distribution in a plane passing through the nanowire axis. The value of the isosurface ranges from 0.06 e/Å^3 (yellow color) to 1.18 e/Å^3 (dark blue). Inset (b) shows the partial charge density isosurface arising from the electronic states in the range of −5.5 to −2.2 eV. It shows charge between Mo and S atoms resulting from p−d hybridization.

However, around I atoms, the charge density is more spread due to its larger size. The charge density is distributed continuously along the nanowire, but there are regions of very low density (voids) along the center of the nanowire. The latter exist in between the Mo_3 triangles. This suggests that charge from this region of the nanowire has been transferred to S or I atoms as well as to the Mo−S bonds.

The band structures for $MoS_{1-x}I_x$ nanowires are shown in Figure 5. The results have been shown for the supercell with 24 atoms. However, for $x = 0$, it corresponds to two unit cells in the z direction and our results for one unit cell agree well with those obtained earlier.[23,26] An important feature of the band structure is the occurrence of three 4d bands that cross the Fermi energy. One band has free electron-like dispersion and arises from the t_{2g} type d_{zx} and d_{yz} orbitals (see Figure S3 in Supporting Information), which are well connected in the infinite chain. Therefore, these bands contribute to electronic transport in the nanowires. The calculated Fermi velocity is 5.74×10^3 m/s. As iodine is doped, the rotational symmetry of the nanowire is broken and the bands shift downward, leading to their higher occupation. Further it can be seen that, for $x = 8.3\%$, there is only one band that crosses the E_F and it is reflected in DOS (see Figure 3). This is likely to reduce the electronic conduction in this nanowire, as transport properties depend on the number of channels. For further iodine doping ($x = 16.7\%$), the E_F crosses a narrow band that gets partially occupied, and it is nearly filled at $x = 25\%$. Another interesting feature arises for $x = 33.3\%$. In this case, the broad band (free electron-like) has only a few holes that would contribute predominantly to conduction. Another higher-lying band falls just below the E_F and will contribute to electron conduction. However, this contribution is expected to be less due to the higher effective electron mass in the narrow band. The calculated Fermi velocity for this band is $\sim 8.4 \times 10^2$ m/s, which is much smaller than that for the broader band.

The energy bands in the cases of higher iodine doping also change significantly, and this is reflected in the DOS curves in Figure 3. It is worth mentioning that although all the nanowires discussed here are metallic, there is a small gap around 0.6 eV at the gamma point for $x = 25\%$, and it

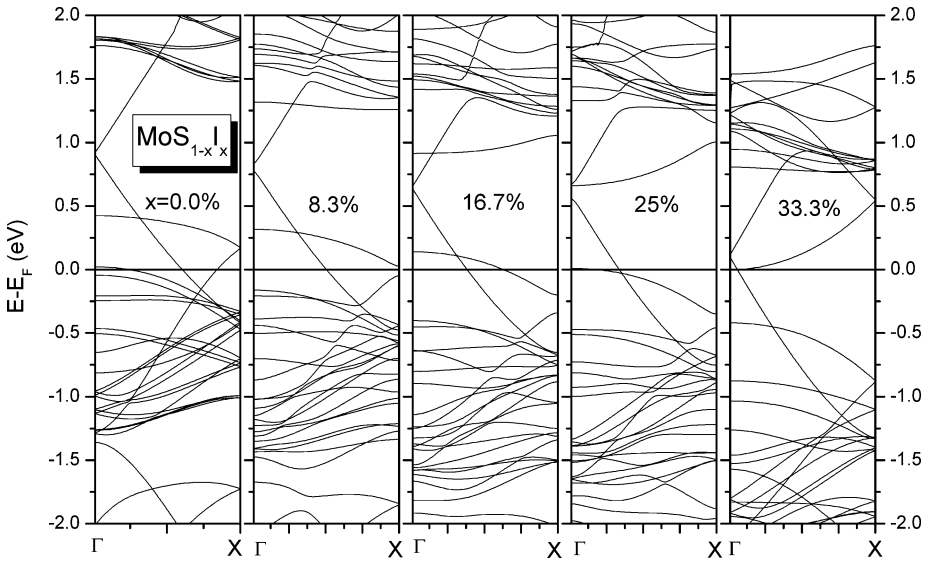

Figure 5. Band structures for infinite $MoS_{1-x}I_x$ nanowires with $x = 0$, 8.3, 16.7, 25, and 33.3%. The successive occupation of the higher lying bands due to iodine doping as well as modifications in hybridization can be seen.

may become possible to perform band gap engineering on these nanowires by suitable doping and substitutions to convert them also in to a semiconductor. Note that MoTe nanowire has been shown to be semiconducting.[27] Also, the MoS nanowires have higher mechanical stability compared with nanowires of Mo_2S_3 stoichiometry. To check the energetic stability of MoS type nanowires, we performed calculations on $Mo_2S_{3-x}I_x$ nanowires, which have been produced experimentally. The BE of $Mo_2S_{3-x}I_x$ nanowires is much lower than the value for the MoS nanowire, as shown in Table S1 (Supporting Information). We therefore believe that MoS nanowires would have superior properties, and it is hoped that in future experiments it may become possible to produce nanowires with compositions considered here.

Summary. In summary, we have shown that an octahedral Mo_6S_8 cluster and linear structures formed from such condensed clusters have high stability compared with other polyhedral forms. This supports the occurrence of finite nanowire-like Mo−S clusters in some compounds. The currently known $Mo_6S_3I_6$ nanowires also have octahedral units that are connected by S/I atoms. However, condensed octahedral units are energetically more favorable. The strong stability of such condensed clusters arises due to Mo−Mo bonding and p−d hybridization. We find that the nanowires with $MoS_{1-x}I_x$ compositions as considered here are energetically more favorable than experimentally found $Mo_2S_{3-x}I_x$ nanowires. The electronic structure of the $MoS_{1-x}I_x$ nanowires suggests their metallic nature. Iodine doping is shown to act like an electron donor and leads to significant changes near E_F as unoccupied bands of MoS nanowire get filled up. This can therefore be used to manipulate the electronic properties of the nanowires. All the nanowires studied here are metallic. However for higher iodine doping, the electronic transport has been found to have dominant contribution from holes. We hope that our results would stimulate experimental work to find $MoS_{1-x}I_x$ nanowires.

Acknowledgment. We thank the staff of the Centre for Computational Materials Science at the IMR for their support and the use of the Hitachi SR8000/64 supercomputing facilities. V.K. acknowledge the kind hospitality at the International Frontier Center for Advanced Materials (IFCAM), IMR. The isosurface contours were visualized by XCRYSDEN.[28]

Supporting Information Available: Relaxed structures of face-capped cube Mo_8S_6 and face-capped cuboctahedron $Mo_{12}S_{14}$; ball-and-stick model of the structure $Mo_{12}S_{12-x}I_x$ nanowires in the unit cell; angular momentum decomposed DOS (lm DOS) of Mo-4d orbitals and s−p orbitals for $MoS_{1-x}I_x$ with $x = 25\%$. BE comparison between the $MoS_{1-x}I_x$ and $Mo_2S_{3-x}I_x$ nanowires. This material is available free of charge via the Internet at http://pubs.acs.org.

References

(1) Dresselhaus, M. S.; Dresselhaus, G.; Eklund, P. C. *Science of Fullerenes and Carbon Nanotubes*; Academic Press.: New York, 1995.
(2) Feldman, Y.; Wasserman, E.; Srolovitz, D. J.; Tenne, R. *Science* **1995**, *267*, 222−225.
(3) Tenne, R. *Angew. Chem., Int. Ed.* **2003**, *42*, 5124−5132.
(4) Zhu, Y. Q.; Sekine, T.; Li, Y. H.; Wang, W. X.; Fay, M. W.; Edwards, H.; Brown, P. D.; Fleischer, N.; Tenne, R. *Adv. Mater.* **2005**, *17*, 1500−1503.
(5) Dassenoy, F.; Joly-Pottuz, L.; Martin, J. M.; Vrbanic, D.; Mrzel, A.; Mihailovic, D.; Vogel, W.; Montagnac, G. *J. Eur. Ceram. Soc.* **2007**, *27*, 915−919.
(6) Nicolosi, V.; Nellist, P. D.; Sanvito, S.; Cosgriff, E. C.; Krishnamurthy, S.; Blau, W. J.; Green, M. L. H.; Vengust, D.; Dvorsek, D.; Mihailovic, D.; Compagnini, G.; Sloan, J.; Stolojan, V.; Carey, J. D.; Pennycook, S. J.; Coleman, J. N. *Adv. Mater.* **2007**, *19*, 543.
(7) Nicolosi, V.; Vrbanic, D.; Mrzel, A.; McCauley, J.; O'Flaherty, S.; McGuinness, C.; Compagnini, G.; Mihailovic, D.; Blau, W. J.; Coleman, J. N. *J. Phys. Chem. B* **2005**, *109*, 7124−7133.
(8) Remskar, M.; Mrzel, A.; Skraba, Z.; Jesih, A.; Ceh, M.; Demsar, J.; Stadelmann, P.; Levy, F.; Mihailovic, D. *Science* **2001**, *292*, 479−481.
(9) Zimina, A.; Eisebitt, S.; Freiwald, M.; Cramm, S.; Eberhardt, W.; Mrzel, A.; Mihailovic, D. *Nano Lett.* **2004**, *4*, 1749−1753.

(10) Paglia, G.; Bozin, E. S.; Vengust, D.; Mihailovic, D.; Billinge, S. J. L. *Chem. Mater.* **2006**, *18*, 100−106. Medan, A.; Kodre, A.; Gomilsek, J. P.; Arcon, I.; Vilfan, I.; Vrbanic, D.; Mrzel, A.; Mihailovic, D. *Nanotechnology* **2005**, *16*, 1578−1583.
(11) Yang, T.; Okano, S.; Berber, S.; Tomanek, D. *Phys. Rev. Lett.* **2006**, *96*, 125502.
(12) Vilfan, I.; Mihailovic, D. *Phys. Rev. B* **2006**, *74*, 235411.
(13) Vilfan, I. *Eur. Phys. J. B* **2006**, *51*, 277−284.
(14) Venkataraman, L.; Lieber, C. M. *Phys. Rev. Lett.* **1999**, *83*, 5334−5337.
(15) Potel, M.; Chevrel, R.; Sergent, M.; Armici, J. C.; Decroux, M.; Fischer, O. *J. Solid State Chem.* **1980**, *35*, 286−290.
(16) Kresse, G.; Hafner, J. *J. Phys.: Condens. Matter* **1994**, *6*, 8245−8257.
(17) Vanderbilt, D. *Phys. Rev. B* **1990**, *41*, 7892−7895.
(18) Perdew, J. P.; Chevary, J. A.; Vosko, S. H.; Jackson, K. A.; Pederson, M. R.; Singh, D. J.; Fiolhais, C. *Phys. Rev. B* **1992**, *46*, 6671−6687.
(19) Murugan, P.; Kumar, V.; Kawazoe, Y.; Ota, N. *Phys. Rev. A* **2005**, *71*, 63203; *Chem. Phys. Lett.* **2006**, *423*, 202−207
(20) Murugan, P.; Kumar, V.; Kawazoe, Y.; Ota, N. *J. Phys. Chem. A* **2007**, *111*, 2778−2782.
(21) Picard, S.; Salloum, D.; Gougeon, P.; Potel, M. *Acta Crystallogr., Sect. C: Cryst. Struct. Commun.* **2004**, *60*, I61−I62.
(22) Simon, A., *Angew. Chem., Int. Ed. Engl.* **1981**, *20*, 1−22.
(23) Ribeiro, F. J.; Roundy, D. J.; Cohen, M. L. *Phys. Rev. B* **2002**, *65*, 153401.
(24) Kumar, V.; Kawazoe, Y. *Phys. Rev. B* **2002**, *66*, 144413.
(25) Pauling, L. *The Nature of the Chemical Bond and the Structure of Molecules and Crystals*; University Press: New York, 1940.
(26) Gemming, S.; Seifert, G.; Vilfan, I. *Phys. Status Solidi B* **2006**, *243*, 3320−3324.
(27) Cakir, D.; Durgun, E.; Gulseren, O.; Ciraci, S. *Phys. Rev. B* **2006**, *74*, 235433.
(28) Kokaji, A. *J. Mol. Graphics Modell.* **1999**, *17*, 176. Code available from http://www.xcrysden.org.

NL0706547